Evaluation of Mechanical Properties of Various Nanofibre Reinforced Bis-GMA/TEGDMA Based Dental Composite Resins

N Tokar[1], E Tokar[2], B Mavis[3], O Karacaer[2]

ABSTRACT

Objective: *To investigate the mechanical properties of various mass fractions of Nylon 6 (N6), polymethyl-metacrylate (PMMA) and polyvinylidene-difluoride (PVDF) nanofibres reinforced bisphenol A-glycidyl methacrylate (Bis-GMA) and tri-ethylene glycol dimethacrylate (TEGDMA) based dental composite resins and to evaluate the penetration characteristics of the nanofibres into the resin.*

Methods: *Nylon 6, PMMA and PVDF nanofibres were produced using the electrospinning method. The morphologies of the fabricated nanofibres were evaluated with a scanning electron microscope (SEM). The nanofibres were placed into the resin matrix at different mass fractions (3%, 5% and 7%). The three-point bending test was applied to nanofibre-reinforced dental composite resins and neat resin specimens. The flexural strength (Fs), flexural modulus (E_Y) and work of fracture (WOF) of the groups were found. The analysis of variance was used for the statistical analysis of the acquired data. Tukey's multiple test was performed to compare the Fs, E_Y and WOF means. Fractured surfaces of the samples were observed by SEM, and fracture morphologies were evaluated.*

Results: *Polymethyl-metacrylate nanofibres dissolved in the matrix, and a polymer alloy took place in the matrix. Fibre pull-out and fibre bridging mechanisms were observed by SEM images of the N6 and PVDF nanofibre-reinforced dental composites. The produced nanofibres enhanced the mechanical properties of the dental composite resins.*

Conclusion: *Fibre pull-out and fibre bridging mechanisms on the fractured surfaces of samples may play a key role in the reinforcement of dental composite resins. However, polymer alloy of PMMA nanofibres increased the mechanical properties of the resin matrix.*

Keywords: Dental composite resins, electrospinning, nanofibre-reinforced composites, nanofibres

Evaluación de las propiedades mecánicas de varias resinas compuestas dentales basadas en Bis-GMA/TEGDMA reforzadas con nanofibras

N Tokar[1], E Tokar[2], B Mavis[3], O Karacaer[2]

RESUMEN

Objetivo: *Investigar las propiedades mecánicas de resinas compuestas dentales basadas en bisfenol A-diglicidildimetacrilato (Bis-GMA) y dimetacrilato trietilen-glicol (TEGDMA) refor-*

From: [1]Clinic of Prosthodontics, Tepebasi Oral and Dental Health Hospital, Kecioren, Ankara, Turkey, [2]Department of Prosthodontics, Faculty of Dentistry, Gazi University, Emek, Ankara, Turkey and [3]Department of Mechanical Engineering, Faculty of Engineering, Hacettepe University, Beytepe, Ankara, Turkey.

Correspondence: Dr N Tokar, Tepebasi Oral and Dental Health Hospital, Fatih Cad Cagla Sk, No. 4, Kecioren, Ankara, Turkey. Email: dtnihalpehlivan@gmail.com

 DOI: 10.7727/wimj.2016.243

zadas con nanofibras de fracciones de masa de Nylon 6 (N6), polimetilmetacrilato (PMMA) y fluoruro de polivinilideno (PVDF), y evaluar las características de la penetración de las nanofibras en la resina.

Métodos: *Se produjeron nanofibras de Nylon 6, PMMA y PVDF utilizando el método de electrohilado (electrospinning). Las morfologías de las nanofibras fabricadas fueron evaluadas con un microscopio electrónico de barrido (MEB). Las nanofibras fueron introducidas en la matriz de resina en diferentes fracciones de masa (3%, 5% y 7%). La prueba de flexión de tres puntos fue aplicada a las resinas compuestas dentales reforzadas por nanofibras y a las muestras de resina pura. La resistencia a la flexión (Rf), el módulo de flexión (E_Y) y el trabajo de fractura (WOF) de los grupos fueron halladas. El análisis de varianza se usó para el análisis estadístico de los datos adquiridos. Se realizó la prueba de comparaciones múltiples de Tukey con el propósito de comparar las medidas de Rf, E_Y y WOF. Las superficies fracturadas de las muestras fueron observadas mediante un MEB, y se evaluaron las morfologías de fractura.*

Resultados: *Las nanofibras de polimetilmetacrilato se disolvieron en la matriz, y tuvo lugar una aleación de polímeros en la matriz. Los mecanismos de desprendimiento de fibras y puenteo de fibras fueron observados mediante imágenes de MEB de los compuestos dentales reforzados con nanofibras de N6 y PVDF. Las nanofibras producidas realzaron las propiedades mecánicas de las resinas compuestas dentales.*

Conclusión: *Los mecanismos de desprendimiento de fibras y puenteo de fibras en las superficies fracturadas de las muestras pueden desempeñar un papel clave en el reforzamiento de las resinas de los compuestos dentales. Sin embargo, la aleación polimérica de las nanofibras de PMMA aumentó las propiedades mecánicas de la matriz de resina.*

Palabras clave: Resinas de compuestos dentales, electrohilado, compuestos reforzados con nanofibras, nanofibras

West Indian Med J 2018; 67 (1): 61

INTRODUCTION

Dental composite resins (DCRs) have been widely used to restore teeth for about half a century (1). They have been used to make aesthetic fillings, replace dental amalgam restorations (2) and also fabricate crown and bridge restorations (3). Inorganic fillers, silane coupling agents, initiators, activators and the organic resin matrix material are constituents of a typical DCR. Synthetic polymers can also be added to DCRs (4).

Although DCRs are commonly used in dental practice, enhancement of their properties is still necessary because of their poor mechanical performances and the high polymerization shrinkage of the resin (5, 6). The constituents of a DCR can be modified to improve its mechanical properties (4). Although the addition of inorganic fillers is mainly for reinforcing the resin, they can become the source of failures (7, 8). Inorganic fillers with irregular shapes can act as a stress concentration point in the resin matrix. Crack initiation from that point is more likely, and such cracks can cut through the fillers or spread around them (8).

High-modulus and high-strength fibres and nanofibres have been used to enhance the flexural strength (Fs), flexural modulus (E_Y) and work of fracture (WOF) of DCRs (2). Nanofibres can be used to improve the mechanical properties of resin even at relatively low filler loadings. Expected mechanical properties may be acquired through modifications to the fibres (9, 10). On average, nanofibres can take on more loads from the matrix and therefore facilitate toughening mechanisms better compared to particle fillers. Fibre bridging and fibre pull-out mechanisms play key roles in toughening the DCRs (5, 7, 11, 12).

Among the various nanofibre preparation techniques, drawing (13), template synthesis (14), phase separation (15), self-assembly (16) and electrospinning (7, 17, 18) are the ones that are commonly applied. Electrospinning is a relatively simple and versatile technique for preparing polymeric, ceramic or composite nanofibres (7, 11, 19, 20). In this process, a high voltage electrostatic field is applied between two electrodes, one of which is attached to the collector and the other is attached to the polymer solution (4, 7, 20). In a typical spinning process,

droplets of the polymer solution are ejected from the tip of the spinneret and the jet formed under the effect of electrical field would migrate to the collector (21). While travelling through the air, the solvent evaporates and so dried polymer fibres can be collected as a non-woven mat at a stationary collector (7, 11, 22). Polymer solution parameters (such as polymer concentration and molecular weight, additives and solvent choice) and process parameters (such as voltage, distance between the collector and the needle, flow rate, geometry of spinneret, type of collector, humidity and temperature) can have a complex influence on the resulting morphologies and dimensions of the electrospun nanofibres.

In a few studies, Nylon 6 (N6) and polymethyl-metacrylate (PMMA) nanofibres were used to reinforce the mechanical properties of DCRs (7, 11, 23, 24). The effects of the use of polyvinylidene-difluoride (PVDF) nanofibres for similar purposes have not been studied yet. In this study, N6, PMMA and PVDF nanofibres were produced by using the electrospinning technique, and the effects of reinforcement of bisphenol A-glycidyl methacrylate (Bis-GMA)/tri-ethylene glycol dimethacrylate (TEGDMA) based DCRs with various mass fractions of electrospun N6, PMMA and PVDF nanofibres were evaluated.

MATERIALS AND METHODS

The following were used in the study: Bis-GMA (Sigma-Aldrich Co LLC, Steinheim, Germany) and TEGDMA (Sigma-Aldrich Co LLC) monomers, camphorquinone (CQ; Sigma-Aldrich Co LLC), ethyl-4 N,N'-dimethylamino benzoate (4EDMAB; Sigma-Aldrich Co LLC), N6 (Sigma-Aldrich Co LLC), methyl methacrylate (MMA; Sigma-Aldrich Co LLC), PVDF (Sigma-Aldrich Co LLC), 2-(Dimethylamino) ethyl methacrylate (Sigma-Aldrich Co LLC), benzoyl peroxide (Sigma-Aldrich Co LLC), trifluoro-ethylene (TFE; Merck KGaA, Darmstadt, Germany), N,N-dimethylformamide (DMF; Merck KGaA), and tetrabutylammonium chloride (TBAC; Sigma-Aldrich Co LLC).

Polymethyl-metacrylate was prepared by mixing MMA (Sigma-Aldrich Co LLC) and 0.01% (by weight) benzoyl peroxide (Sigma-Aldrich Co LLC) for nine hours at 60°C.

Production of nanofibres

Nylon 6: electrospinning solution, which was prepared by dissolving 10% (by weight) N6 in TFE, was stirred for 24 hours until a clear liquid was acquired. The solution was then drawn up by 10 ml syringes with metallic needles that had an inner diameter of 0.8 mm. Syringes were inserted horizontally on a syringe pump (NE-1600, New Era Pump Systems Inc, New York, United States of America (USA)).

A high voltage power supply (ES30, Gamma High Voltage Research, Ormond Beach, Florida, USA) was used to apply 15 kV to the metal needle tip. The distance between the needle tip and the collector was set at 25 cm. Nylon 6 nanofibres were deposited on a collector that was covered with electrically grounded aluminum foil.

Polymethyl-metacrylate: PMMA polymer solution was prepared using 10% (by weight) PMMA dissolved in DMF. The mixture was stirred for 24 hours and electrospun at 15 kV with a 20 cm distance between the needle tip and the collector.

Polyvinylidene-difluoride: addition of small quantities of TBAC in the PVDF polymer solutions increased the chance of crystalline phase formations. In addition to decreased beading tendencies, the diameters of the nanofibres could also be decreased (19).

For dissolving PVDF, a DMF-acetone mixture was prepared with a DMF/acetone weight ratio of 60/40.2% (by weight). Tetrabutylammonium chloride was added to the solvent mixture, and 20% (by weight) PVDF polymer was dissolved in this solution. The solution was electrospun at 25 kV with a 16 cm distance between the needle tip and the collector.

All polymer solutions were fed at 1 ml/hour during the electrospinning process. Morphologies of the produced nanofibres were examined by a scanning electron microscope [SEM] (FEI Quanta 400F). Nanofibres from all polymer types were generally uniform in diameter, smooth and bead-free (Fig. 1).

Fabrication of specimens

Composite resin matrix was prepared by mixing 49.5% Bis-GMA, 49.5% TEGDMA, 0.2% CQ and 0.8% 4EDMAB. This also constituted the control group. The fabricated nanofibres were placed into the composite resin matrix at different mass fractions (3%, 5% and 7%) layer by layer. Beam-shaped specimens measuring 2 mm x 2 mm x 25 mm were prepared and photo-cured for two minutes with curing light (QHL 75, Dentsply, Milford, Delaware, USA). Before the mechanical test, the specimens were immersed in distilled water at 37°C for 24 hours. Then, four sides of the specimens were polished in a longitudinal direction with 2400 grit silicon carbide paper using water coolant. With the control group, there

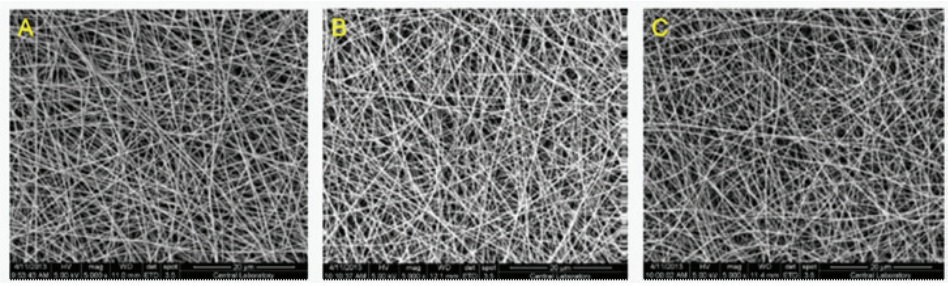

Fig. 1: Scanning electron microscope images of N6 nanofibres (A), PVDF nanofibres (B) and PMMA nanofibres (C).

were 10 different groups and for each group, 10 specimens were prepared and mechanically tested.

Mechanical properties

A three-point bending jig with a 20 mm span was used to fracture the specimens on a computer-controlled Universal Testing Machine (LRX, Lloyd Instruments Ltd, Fareham Hants, England) at a cross-head speed of 1 mm/minute to record stress strain curves. Ten specimens were tested in each group, and the Fs, E_Y and WOF of nanofibre-reinforced Bis-GMA/TEGDMA composites were found. Calculations were made using the following formulae: $Fs = 3PL / 2WT^2$; $E_Y = (P / d) (L^3 / 4WT^3)$; $WOF = A / (WT)$, where P is the load at fracture, L is the distance between two supports (which was set to be 20 mm), W is the width of the specimen, T is the thickness of the specimen, and d is the deflection (in mm) at load P. In the formula of WOF, A is the area under the load-displacement curve, which is the work done by the applied load to deflect and fracture the specimen. The unit of WOF (or fracture resistance) is J/m^2 or, more conveniently, kJ/m^2.

The analysis of variance was used for the statistical analysis of the acquired data. Tukey's multiple test was used to compare the Fs, E_Y and WOF means, and significant levels were considered at p-values ≤ 5. The level of confidence was established at $\alpha = 5\%$. Statistical analysis was performed using statistical package SPSS 11.5 for Windows (SPSS Inc, Chicago, USA). The fractured surfaces of the specimens were coated with carbon (about 5 nm) and observed with SEM.

RESULTS

Different mass fractions of the N6, PMMA and PVDF nanofibre-reinforced Bis-GMA/TEGDMA dental composite (NRDC) specimens were tested using a standard three-point bending test method. The mechanical properties of Fs, E_Y and WOF of the specimens were calculated and evaluated *via* statistical analysis. In addition, fractured surfaces of the specimens were inspected using SEM analysis.

Influence of the type of nanofibre on the mechanical properties of the resin

The Table shows the Fs, E_Y and WOF results of different mass fractions of the NRDCs.

Tukey's honest significant difference (HSD) statistical analysis of the Fs results showed the differences among the groups. Accordingly, 5% N6, 3% and 5% PMMA, and 5% and 7% PVDF NRDC groups showed higher Fs results compared to those of the control group. These differences were found to be statistically significant ($p < 0.05$). The 3% PMMA NRDC group showed a better Fs result than that of the 3% PVDF NRDC group, and the difference between the groups was statistically significant ($p < 0.05$). The Fs result of the 7% PVDF NRDC group was statistically significantly higher than that of the 7% N6 NRDC group [$p < 0.05$] (Fig. 2).

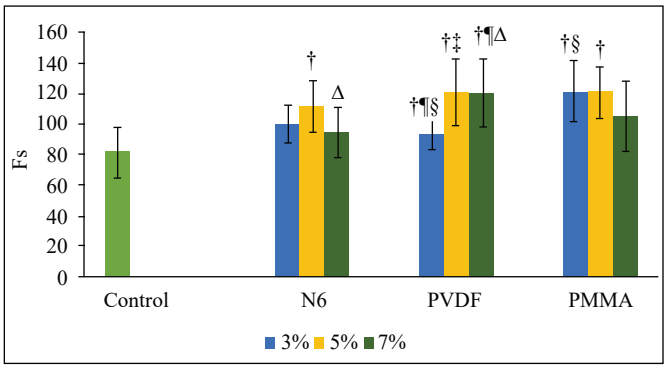

Fig. 2: Multiple comparisons of Fs results. Similar symbols show statistically significant differences between the groups.

Tukey's HSD statistical analysis of the E_Y results indicated that the 3%, 5% and 7% PMMA NRDC groups were significantly different from the control group ($p < 0.05$). The E_Y results of the N6 and PVDF NRDC groups were increased, but this was not statistically significant ($p \geq 0.05$). The E_Y result of the 3% PMMA NRDC group was statistically different compared to those of the 3%

Table: Descriptive statistical analysis of Fs, Ey and WOF results

	Group	n	Mean	Standard deviation	Standard error	95% confidence interval for mean		Minimum	Maximum
						Lower bound	Upper bound		
Fs	Control	10	82.12	16.57	5.24	70.26	93.97	52.57	108.62
	3% N6	10	100.19	12.32	3.90	91.38	109.01	86.54	119.41
	5% N6	10	112.20	17.42	5.51	99.74	124.66	90.03	135.66
	7% N6	10	94.60	16.24	5.14	82.98	106.22	77.32	133.77
	3% PVDF	10	94.12	9.78	3.09	87.13	101.11	80.80	107.85
	5% PVDF	10	120.79	21.97	6.95	105.08	136.51	91.96	155.19
	7% PVDF	10	120.85	22.25	7.04	104.93	136.77	86.68	151.35
	3% PMMA	10	121.69	19.70	6.23	107.59	135.78	88.86	150.13
	5% PMMA	10	121.03	16.43	5.19	109.28	132.79	99.50	153.54
	7% PMMA	10	105.49	23.06	7.29	88.99	121.98	75.16	146.78
	Total	100	107.31	21.88	2.19	102.97	111.65	52.57	155.19
Ey	Control	10	2187.78	736.08	232.77	1661.22	2714.34	1276.77	3668.95
	3% N6	10	2573.52	375.89	118.87	2304.63	2842.43	2058.04	3236.68
	5% N6	10	2976.53	594.31	187.94	2551.39	3401.68	2087.68	3848.79
	7% N6	10	2224.89	535.79	169.43	1841.61	2608.17	1642.95	3402.89
	3% PVDF	10	2581.49	521.30	164.85	2208.57	2954.40	1767.24	3310.38
	5% PVDF	10	2858.02	917.60	290.17	2201.61	3514.43	1683.17	4853.48
	7% PVDF	10	2616.94	410.95	129.95	2322.96	2910.92	1658.42	3314.01
	3% PMMA	10	3607.33	824.40	260.70	3017.58	4197.07	2663.15	4694.99
	5% PMMA	10	3223.22	680.84	215.30	2736.17	3710.27	2684.57	5037.05
	7% PMMA	10	3341.00	379.56	120.03	3069.48	3612.52	2802.03	3917.28
	Total	100	2819.07	745.12	74.51	2671.22	2966.92	1276.77	5037.05
WOF	Control	10	4.08	1.68	0.53	2.88	5.28	1.68	7.09
	3% N6	10	5.13	1.45	0.46	4.09	6.16	3.10	7.96
	5% N6	10	5.82	2.16	0.68	4.28	7.36	3.07	9.23
	7% N6	10	5.48	1.48	0.47	4.42	6.54	3.09	7.73
	3% PVDF	10	4.22	0.98	0.31	3.52	4.92	2.66	6.25
	5% PVDF	10	7.39	3.50	1.11	4.88	9.89	3.37	14.96
	7% PVDF	10	7.72	2.52	0.80	5.92	9.52	4.40	12.40
	3% PMMA	10	5.56	2.75	0.87	3.59	7.53	1.85	9.97
	5% PMMA	10	6.19	2.52	0.80	4.39	7.99	3.63	11.59
	7% PMMA	10	4.41	2.43	0.77	2.67	6.14	1.73	8.59
	Total	100	5.60	2.46	0.25	5.11	6.09	1.68	14.96

N6 and 3% PVDF NRDC groups, and these differences were statistically significant ($p < 0.05$). The E_Y result of the 7% PMMA NRDC group was found to be significantly higher than that of the 7% N6 NRDC group [$p < 0.05$] (Fig. 3).

Tukey's HSD statistical analysis of the WOF results showed that the 5% and 7% PVDF NRDC groups were significantly higher than the control group ($p < 0.05$). The WOF results of the other groups were increased compared to the control group, but these were not statistically significant. The WOF result of the 7% PVDF NRDC group was found to be statistically significantly better than the 7% PMMA NRDC group [$p < 0.05$] (Fig. 4).

Influence of the nanofibre ratio on the mechanical properties of the resin

Tukey's HSD test was performed to determine the effect of the nanofibre ratio. The Fs values of the 5% and 7% PVDF NRDC groups were significantly increased with respect to the 3% PVDF NRDC [$p < 0.05$] (Fig. 2). Differences among the various mass fractions of the N6 and PMMA NRDC groups were not found to be statistically significant ($p \geq 0.05$).

The E_Y results of the various mass fractions of nanofibre addition showed different values, but these were not determined to be statistically significant [$p \geq 0.05$] (Fig. 3).

The WOF result of the 7% PVDF NRDC group was found to be higher than that of the 3% PVDF NRDC group (Fig. 4). The WOF results of the various mass fractions of the N6 and PMMA NRDC groups were different, but these results were not found to be statistically significant ($p \geq 0.05$).

Analysis of the specimens by a scanning electron microscope

The fracture surfaces of the specimens were evaluated with a SEM. The fracture surfaces of the control group (neat resin) were smooth and observed with fewer fracture steps (Fig. 5A).

Resin matrix was observed to be well penetrated into the N6 nanofibre layers and interspaces. In addition, N6 nanofibres retained their integrity and morphology in the resin matrix (Figs. 5B, 5C, 5D).

The PVDF nanofibres demonstrated clear evidence of an active fibre pull-out mechanism on the fractured surfaces. Besides, the PVDF nanofibres remained integral and showed no signs of dissolution into the resin matrix (Figs. 5E, 5F, 5G).

Observations by a SEM of the fractured surfaces of the PMMA NRDC groups showed that the PMMA nanofibres lost their integrity since they dissolved almost completely in the matrix monomer. Fibre layers were identified more explicitly in the 5% and 7% PMMA NRDC groups compared to the 3% PMMA NRDC group (Figs. 5H, 5I, 5J).

DISCUSSION

Since the 1960s, clinicians have frequently used DCRs as a restorative material (8, 11). Dental composite resins have many advantages, such as being biocompatible,

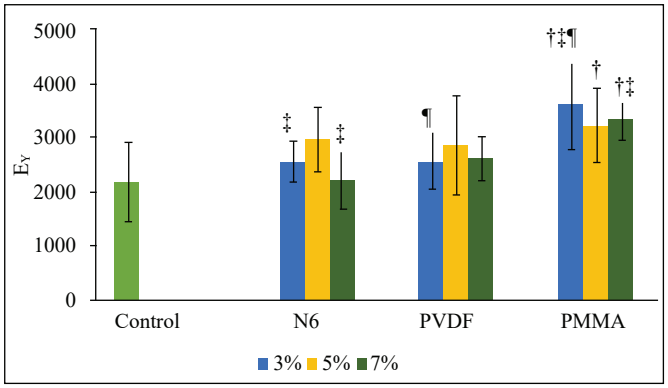

Fig. 3: Multiple comparisons of EY results. Similar symbols show statistically significant differences between the groups.

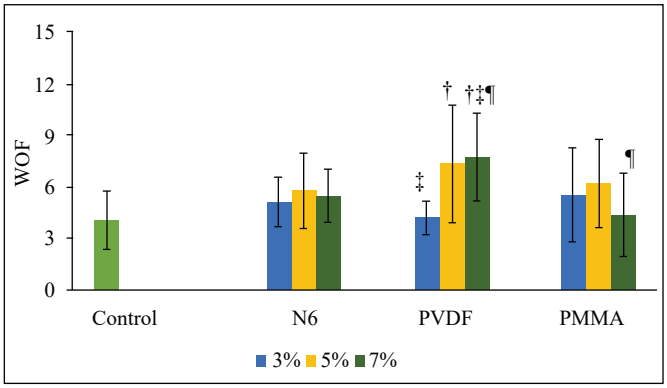

Fig. 4: Multiple comparisons of WOF results. Similar symbols show statistically significant differences between the groups.

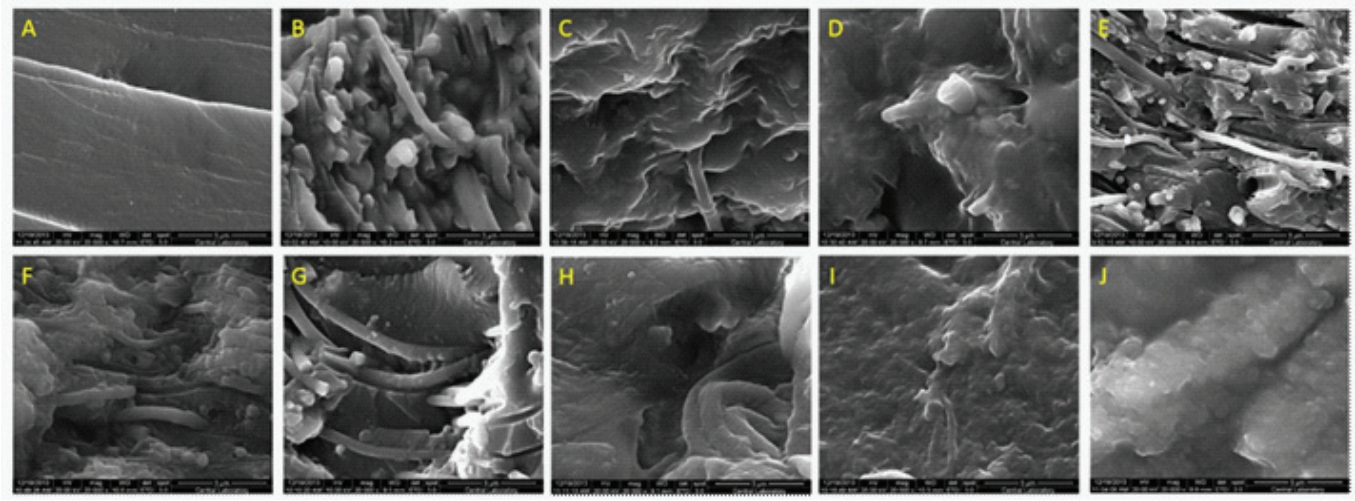

Fig. 5: Scanning electron microscope images of fractured surfaces (x 20 000 magnification): control group (A), 3% N6 NRDC group (B), 5% N6 NRDC group (C), 7% N6 NRDC group (D), 3% PVDF NRDC group (E), 5% PVDF NRDC group (F), 7% PVDF NRDC group (G), 3% PMMA NRDC group (H), 5% PMMA NRDC group (I), 7% PMMA NRDC group (J).

aesthetic and cost-efficient. However, they still need to be improved mechanically, physically and biologically for successful long-term restorations. The main components of DCRs, especially inorganic fillers, can be modified to enhance mechanical properties (4). Thus, glass or ceramic particles, glass fibres, whiskers, nanotubes and nanofibres have been added into the resins (7, 8).

The nanofibres were found to be effective in reinforcing the mechanical properties of the DCRs in the last decade. They have a high surface area to volume ratio, small pore dimensions, very good interfacial properties, strong adhesion to the matrix and other fillers, and can promote crack bridging mechanisms (9, 25, 26). Hence, a small amount of nanofibre addition can improve the mechanical properties of the DCRs significantly (9). The cylindrical and agonic morphologies of the nanofibres prohibit the generation of stress concentration points (8, 11). Crack formations can also be prevented due to activated crack bridging mechanisms. When microcracks occur in the resin matrix, nanofibres that remain sound in the crack propagation lines can resist the forces and deflect the cracks. By this way, crack propagation would necessitate higher energies. Therefore, a resin matrix can be reinforced by the crack bridging nanofibres, and opening of the cracks can be decreased (2).

Electrospinning is a simple, suitable and versatile method for the production of polymer, ceramic and metal nanofibres (26). Bending instability is the key phenomenon of the electrospinning method. The jet can be elongated up to 100 000 times in less than 0.1 second, and the shape of the jet resembles an expanding coil (27). This high aspect draw ratio can generate extended chains. The formation of polymer crystallites can be controlled (7). For example, during the electrospinning of PVDF nanofibres, β-phase formation can be triggered with small additions of TBAC in the polymer solution. In addition, the morphologies and diameters of the nanofibres can be controlled, and bead formation of the fibres may be prevented (19).

The mechanical properties of PVDF nanofibre-reinforced DCRs had not been examined previously. In this study, various mass fractions of PVDF nanofibres were placed layer by layer in the Bis-GMA/TEGDMA-based resin matrix to study the possible mechanical improvements that can be attained by the use of PVDF nanofibres in DCRs. In addition, N6 and PMMA nanofibres were fabricated using the electrospinning method, and 3%, 5% and 7% NRDCs were prepared in the same way. The mechanical properties of the NRDCs were evaluated using three-point bending test results.

Fong evaluated the mechanical properties of N6 NRDC with various mass fractions (7). The 5% N6 NRDC group showed a significant increase in the mechanical properties compared to the 2.5% N6 NRDC group. The 7.5% N6 NRDC group did not show a significant increase. This was explained by insufficient adhesion between the resin matrix and nanofibres. Fong supported the explanation by SEM images from fracture surfaces which showed pulled-out nanofibres that had no resin remnants on their surface. The control group showed large fracture steps, while in the N6 NRDC groups, many fracture steps were seen.

Tian *et al* (11) investigated the mechanical properties of N6 NRDC resin. They had put 1%, 2%, 4% and 8% mass fractions of N6 nanofibres into the resin matrix. They reported that 1% and 2% N6 nanofibres successfully reinforced the DCR, but 4% and 8% N6 nanofibres did not improve the mechanical properties significantly. They explained that the use of high ratios of nanofibres could cause an increase in defect formation between the nanofibre and the matrix, and this negatively affected the nanofibre bonding to the matrix.

Core-shell nanofibres could be used to improve the mechanical properties of DCRs. The aim of the use of this type of nanofibre is to enhance adhesion between the shell and the resin matrix, and to reinforce the DCR *via* a strong core (8, 23, 24). Lin *et al* produced polyacrylonitrile (PAN) core-PMMA shell nanofibre to strengthen the mechanical properties of the DCRs (8). They compared the Fs, E_Y and WOF results of PAN, PMMA and PAN-PMMA NRDCs with 2.5%, 5%, 7.5% and 10% mass fractions. The mechanical properties of the PMMA NRDC groups were found to be lower than those of the control group.

Electrospun nanofibres can be aligned to improve the mechanical properties of the resin further. A post-drawing treatment can enhance the degree of nanofibre alignment and crystallinity of the polymer as well (28). Sun *et al* conducted a PAN core-PMMA shell NRDC study in order to evaluate the mechanical properties of NRDCs (24). They treated PAN-PMMA nanofibres using a post-drawing process. They compared the mechanical effects of PAN-PMMA and post-drawn PAN-PMMA. Analysis by a SEM of the fracture surfaces showed that post-drawn PAN-PMMA nanofibres were perfectly bonded to the resin matrix. Semi-interpenetrating network formation ensured good adhesion between the two

structures. Therefore, post-drawn PAN-PMMA showed better mechanical properties compared to PAN-PMMA NRDCs. Sun *et al* also stated that the post-drawing process enhanced the parallelism and alignment of nanofibres which also had an additional improvement effect on the mechanical properties of the DCRs. Apart from that, 1.2% PAN-PMMA NRDC showed better mechanical properties against 1.6% PAN-PMMA NRDC. This effect was explained by the possibility of having more defects in higher nanofibre additions.

Cheng *et al* aimed to reinforce DCRs with sodium fluoride (NaF) loaded PAN (core)-PMMA (shell) nanofibres (23). They added 0.8% and 1% nanocrystalline NaF to the core of the PAN-PMMA nanofibres and reported that this loading process did not damage the core-shell structure of the PAN-PMMA nanofibres. On the other hand, superior adhesion between the resin matrix and nanofibres improved the mechanical properties of the DCR. Apart from that, NaF-loaded PAN-PMMA nanofibres can have the added benefit of releasing fluoride that prevents caries. The electrospinning process of the NaF-loaded PAN-PMMA nanofibre affected the thickness of the shell, and the release rate of the fluoride decreased when the thickness of the shell was increased. Cheng *et al* also reported that an increase in the shell thickness decreased the mechanical properties of the resin.

Polymethyl-metacrylate nanofibres are known to dissolve partially with the methacryloyl groups on the Bis-GMA main chain, and the nanofibres can lose their fibre morphology in such a matrix (8, 24). Therefore, in this study, a small amount of nanofibres were observed in SEM images of fracture surfaces in the PMMA group. When the PMMA nanofibre ratio is more than the dissolution capacity of the resin, PMMA fibres can start to stick together (8).

Chen *et al* investigated the mechanical properties and water absorption behaviour of DCR containing glyoxylic acid (GA) modified with high-aspect ratio hydroxyapatite (HAP) nanofibres (29). They found that GA modified high-aspect ratio HAP nanofibres were dispersed better than neat HAP nanofibres in the resin matrix. Thus, this circumstance led to greater biaxial Fs. Glyoxylic acid modified HAP nanofibres increased the water absorption and solubility of the DCR. They concluded that this type of nanofibre was not appropriate for clinical use.

Zirconia nanofibres can be used to reinforce Bis-GMA-based composite resins. Xu *et al* put zirconia-yttrium, zirconia-silica and zirconia-yttrium-silica nanofibres into the resin matrix (30). They produced non-porous and dense nanofibres, and the diameter of the fibres changed between 100 nm and 300 nm. Besides, the surface of zirconia-based nanofibres was suitable for bonding to the silica particles. These specifications of the nanofibres ensured improvement of the mechanical properties. Guo *et al* produced zirconia-silica and zirconia-yttrium NRDCs that showed greater mechanical properties compared to the neat resin, except in the 7.5% zirconia-silica NRDC group (2).

In the present study, the mechanical properties of DCR with N6 nanofibres were improved, but the mechanical properties of the 7% N6 NRDC group did not show an increase compared to the 3% and 5% N6 NRDC groups. This result was similar to those in the studies by Fong (7) and Tian *et al* (11). Signs of the fibre pull-out mechanism and fracture steps were observed in the SEM micrographs of fracture surfaces of the N6 NRDC groups. The fracture steps indicated resistance to the applied force. Therefore, the nanofibres were effective in deflecting the cracks (7).

The Fs, E_Y and WOF results of the PMMA NRDC groups were found to be better than those of the control group. These results were different from those of Lin *et al* (8). The E_Y and Fs results of the 5% PMMA NRDC group were lower than those of the 3% PMMA NRDC group. Increasing the mass fraction of the nanofibre can lead to defect formation which obviously weakens the composite. Polymethyl-metacrylate nanofibres were dissolved into the resin matrix, and they lost their fibre morphologies. In this configuration, this group of samples could be considered as a ‘polymer alloy’ in the present study. A few PMMA nanofibres were seen in the SEM images of fracture surfaces, and they were stuck together because of about-to-dissolve nanofibres. Cheng *et al* (23) and Sun *et al* (24) had observed the same phenomena for PMMA nanofibres.

In the current study, PVDF nanofibres were added to the DCR, and the mechanical properties were found to be better than those of the control group. The Fs result from the 7% PVDF NRDC group was higher compared to that from the N6 NRDC group. The WOF result of the same group was also significantly higher than that of the 7% PMMA NRDC group. The mechanical properties of the 5% PVDF NRDC group were better than those of the 3% PVDF NRDC group, but an addition of 7% PVDF nanofibre did not improve the DCR significantly. The Bis-GMA monomer did not dissolve PVDF nanofibres, and they were observed to be intact in SEM images. The fibre pull-out mechanism played an important role in the reinforcement with PVDF nanofibres.

In this study, N6, PVDF and PMMA nanofibres were placed successfully into the Bis-GMA/TEGDMA-based resin matrix. Mechanical test results showed that produced nanofibres improved the mechanical properties of DCRs. An increase in nanofibre mass fractions led to more defect formations and so reinforcement at those fractions was not statistically significant. Polymethylmetacrylate nanofibres dissolved in the methacryloyl groups on the Bis-GMA main chain and lost their fibre integrity partly or completely. However, the resulting mechanical properties of this polymer alloy were found to be higher than the neat resin. Fibre pull-out and fibre bridging mechanisms can play a key role in the improvement of DCRs with nanofibres. The existence of an active fibre pull-out mechanism was observed in the SEM images of the fracture surfaces of PVDF DCRs. The results of this study suggested that a mechanical improvement was possible for Bis-GMA/TEGDMA-based DCRs that could be used in dental restorations. However, further analysis is needed to approve the clinical usage of NRDCs.

ACKNOWLEDGEMENTS

This research was supported by the Gazi University Scientific Research Projects Unit (project no: 03/2011/31), Turkey.

REFERENCES

1. Bowen RL. Properties of a silica-reinforced polymer for dental restorations. J Am Dent Assoc 1963; **66:** 57–64.
2. Guo GQ, Fan YW, Zhang JF, Hagan JL, Xu XM. Novel dental composites reinforced with zirconia-silica ceramic nanofibers. Dent Mater 2012; **28:** 360–8.
3. Sakoguchi K, Minami H, Suzuki S, Tanaka T. Evaluation of fracture resistance of indirect composite resin crowns by cyclic impact test: influence of crown and abutment materials. Dent Mater J 2013; **32:** 433–40.
4. Chen MH. Update on dental nanocomposites. J Dent Res 2010; **89:** 549–60.
5. Chen L, Yu Q, Wang Y, Li H. BisGMA/TEGDMA dental composite containing high aspect-ratio hydroxyapatite nanofibers. Dent Mater 2011; **27:** 1187–95.
6. Sarrett DC. Clinical challenges and the relevance of materials testing for posterior composite restorations. Dent Mater 2005; **21:** 9–20.
7. Fong H. Electrospun nylon 6 nanofiber reinforced BIS-GMA/TEGDMA dental restorative composite resins. Polymer 2004; **45:** 2427–32.
8. Lin S, Cai Q, Ji JY, Sui G, Yu YH, Yang XP et al. Electrospun nanofiber reinforced and toughened composites through in situ nano-interface formation. Compos Sci Technol 2008; **68:** 3322–9.
9. Schaefer DW, Justice RS. How nano are nanocomposites? Macromolecules 2007; **40:** 8501–17.
10. Van Heumen CC, Kreulen CM, Bronkhorst EM, Lesaffre E, Creugers NH. Fiber reinforced dental composites in beam testing. Dent Mater 2008; **24:** 1435–43.
11. Tian M, Gao Y, Liu Y, Liao Y, Xu R, Hedin NE et al. Bis-GMA/TEGDMA dental composites reinforced with electrospun nylon 6 nanocomposite nanofibers containing highly aligned fibrillar silicate single crystals. Polymer 2007; **48:** 2720–8.
12. Xu HH, Schumacher GE, Eichmiller FC, Peterson RC, Antonucci JM, Mueller HJ. Continuous-fiber preform reinforcement of dental resin composite restorations. Dent Mater 2003; **19:** 523–30.
13. Ondarcuhu T, Joachim C. Drawing a single nanofibre over hundreds of microns. Europhys Lett 1998; **42:** 215–20.
14. Martin CR. Membrane-based synthesis of nanomaterials. Chem Mater 1996; **8:** 1739–46.
15. Ma PX, Zhang RY. Synthetic nano-scale fibrous extracellular matrix. J Biomed Mater Res 1999; **46:** 60–72.
16. Liu GJ, Ding JF, Qiao LJ, Guo A, Dymov BP, Gleeson JT et al. Polystyrene-block-poly (2-cinnamoylethyl methacrylate) nanofibers – preparation, characterization, and liquid crystalline properties. Chem-Eur J 1999; **5:** 2740–9.
17. Fong H, Reneker DH. Electrospinning and formation of nanofibers. In: Salem DR, ed. Structure formation in polymeric fibers. Munich: Hanser; 2001.
18. Bhardwaj N, Kundu SC. Electrospinning: a fascinating fiber fabrication technique. Biotechnol Adv 2010; **28:** 325–47.
19. Yee WA, Kotaki M, Liu Y, Lu XH. Morphology, polymorphism behavior and molecular orientation of electrospun poly(vinylidene fluoride) fibers. Polymer 2007; **48:** 512–21.
20. Huang ZM, Zhang YZ, Kotaki M, Ramakrishna S. A review on polymer nanofibers by electrospinning and their applications in nanocomposites. Compos Sci Technol 2003; **63:** 2223–53.
21. Chronakis IS. Novel nanocomposites and nanoceramics based on polymer nanofibers using electrospinning process – a review. J Mater Process Tech 2005; **167:** 283–93.
22. Fong H, Chun I, Reneker DH. Beaded nanofibers formed during electrospinning. Polymer 1999; **40:** 4585–92.
23. Cheng L, Zhou X, Zhong H, Deng X, Cai Q, Yang X. NaF-loaded core-shell PANPMMA nanofibers as reinforcements for Bis-GMA/TEGDMA restorative resins. Mater Sci Eng C Mater Biol Appl 2014; **34:** 262–9.
24. Sun W, Cai Q, Li P, Deng X, Wei Y, Xu M et al. Post-draw PAN-PMMA nanofiber reinforced and toughened Bis-GMA dental restorative composite. Dent Mater 2010; **26:** 873–80.
25. Gao Y, Sagi S, Zhang LF, Liao YL, Cowles DM, Sun YY et al. Electrospun nano-scaled glass fiber reinforcement of Bis-GMA/TEGDMA dental composites. J Appl Polymer Sci 2008; **110:** 2063–70.
26. Nayak R, Padhye R, Kyratzis I, Truong YB, Arnold L. Recent advances in nanofibre fabrication techniques. Text Res J 2012; **82:** 129–47.
27. Reneker DH, Yarin AL, Fong H, Koombhongse S. Bending instability of electrically charged liquid jets of polymer solutions in electrospinning. J Appl Phys 2000; **87:** 4531–47.
28. Zong X, Ran S, Kim KS, Fang D, Hsiao BS, Chu B. Structure and morphology changes during in vitro degradation of electrospun poly(glycolide-co-lactide) nanofiber membrane. Biomacromolecules 2003; **4:** 416–23.
29. Chen L, Xu CQ, Wang Y, Shi J, Yu QS, Li H. BisGMA/TEGDMA dental nanocomposites containing glyoxylic acid-modified high-aspect ratio hydroxyapatite nanofibers with enhanced dispersion. Biomed Mater 2012; **7:** 045014.
30. Xu X, Guo G, Fan Y. Fabrication and characterization of dense zirconia and zirconiasilica ceramic nanofibers. J Nanosci Nanotechnol 2010; **10:** 5672–9.